Mon. Not. R. Astron. Soc. **000**, 1–16 (2001) Printed 1 February 2008 (MN LATEX style file v2.2)

Irradiation Pressure Effects in Close Binary Systems

S. Phillips and Ph. Podsiadlowski*
University of Oxford, Nuclear and Astrophysics Laboratory, Oxford, OX1 3RH, England

1 February 2008

ABSTRACT

We present a method for the calculation of the effects of external irradiation on the geometrical shape of the secondary in a close binary containing a compact star, the source of the radiation, and a normal companion star, where we include the possibility of shadowing by an accretion disc. The model is based on a simple modification of the standard Roche binary potential in which the radiation-pressure force is parameterised using the ratio of the radiation to the gravitational force. We have constructed numerical solutions of approximate 3-dimensional irradiated equipotential surfaces to demonstrate the main geometrical effects of external radiation pressure. For systems in which the inner Lagrangian point is irradiated directly and for sufficiently high irradiation fluxes, the critical condition for which the secondary fills its tidal lobe changes from an inner to an outer critical configuration, where the critical equipotential surface connects to one of the outer rather than the inner Lagrangian point. Such a situation may apply to evaporating binary pulsar systems (e.g. PSR 1957+20), stars orbiting supermassive black holes in AGN and some high-mass X-ray binaries (including Centaurus X-3). For systems containing an accretion disc, which shadows the inner Lagrangian point from the external irradiation, the presence of significant radiation pressure causes a non-axisymmetric deformation of the stellar surface. This has particularly important consequences for low-mass X-ray binaries, for which the X-ray luminosities can be close to the Eddington limit. We have calculated modified Roche potentials to determine the main effects on the optical lightcurves and radial velocity curves for typical binary parameters. Compared to previous studies, the inclusion of irradiation-pressure effects results in changes in the derived system parameters (e.g. component masses, radial velocities) that may be as high as ~ 30 per cent. We conclude that the proper inclusion of irradiation pressure effects is essential for a reliable analysis of close binary systems in which the secondaries are strongly being irradiated.

Key words:
binaries: close – stars: neutron – X-rays: stars – radiative transfer — pulsars: PSR 1957+20 — stars: Centaurus X-3

1 INTRODUCTION

Irradiation of the secondaries in close binary systems can significantly change their appearance and even their internal structure. These are particularly dramatic in the case of low-mass X-ray binaries, in which the luminosity of the compact object can be as high as $10^{38}\,\mathrm{erg\,s^{-1}}$ (i.e. close to the Eddington luminosity of a neutron star), and where the luminosity intercepted by the secondary may be several orders of magnitude larger than the internal luminosity. Depending on the structure and chemical composition of the stellar atmosphere, a fraction of the incident radiation will be absorbed, thereby heating material in the region of penetration. Some of the luminosity deposited in the secondary will be re-radiated at lower wavelengths, increasing the outward flux and raising the surface temperature. The rest will move to cooler regions of the surface via circulation currents. This leads to a change in the temperature and entropy profiles of the envelope. The former will affect the emitted flux, altering the phase-dependent lightcurve. It will also cause a variation in the temperature gradient, which can modify the spectral line profiles and, in turn, the radial velocity curves determined from spectral lines. The change in the entropy in the layer where the irradiation flux is thermalised may influence the long-term equilibrium structure of the star and can, under certain conditions, lead to significant expansion (Podsiadlowski 1991).

Many of these effects have been addressed by a number

* E-mail: podsi@astro.ox.ac.uk

of authors in the past (see, for example, reviews by Peraiah 1982; Kopal 1988; van Paradijs 1998; and also Davey & Smith 1992; Martin & Davey 1995). The purpose of the present study is to investigate an associated, but often neglected effect of irradiation: the pressure force due to the momentum transfer of the incident photons. This is particularly important for X-ray binaries in which the radiation pressure force acting on the secondary may be a substantial fraction of the gravitational force. The consequences of this can be quite dramatic, sometimes involving a large deformation of the secondary's surface and a possible shift in the position of the effective inner Lagrangian point L_1. In extreme cases, mass loss from the secondary can occur through one of the outer Langrangian points, L_2 or L_3, rather than the inner one. Irradiation can then drastically change the dynamics of mass transfer and the nature of the binary interaction.

Standard procedures for the modelling of photometric lightcurves of close binary systems and most models for binary interactions are based on the Roche model for the equipotential surfaces of the binary components. This assumes that both components are centrally concentrated and that their gravitational effects can be approximated as those of point masses. The Roche model has been extended by various authors to overcome some of the intrinsic approximations of circular orbits and synchronous rotation (e.g. Plavec 1958; Kruszewski 1966). In addition, tidal and rotational distortions, the reflection effect, limb- and gravity-darkening can all be treated in a reasonably physical manner (e.g. Kopal 1959; Al Naimiy, 1978.). However, the classical Roche model allows only for gravitational and centrifugal forces, and no provision is made for systems in which external radiation pressure acting on either component is important.

In this paper we present a systematic investigation of the effects of external irradiation pressure on the standard model of binary stellar surfaces. In section § 2 we justify the approach and in § 3 we show how the Roche-lobe model can be modified to approximately include the effects of external irradiation. In § 4 we describe the numerical procedure used to construct these approximate irradiated equipotential surfaces. Binary systems with and without accretion discs are considered, and the validity of our solutions for given parameters will be examined. In § 5 and § 6, we apply these solutions to a number of physical phenomena and systems, with and without accretion discs, respectively. In particular, we discuss applications to binary pulsars, systems with extreme mass ratios and low- and high-mass X-ray binaries.

2 THE RADIATION-PRESSURE FORCE TERM

Radiation pressure is caused by the interaction between electromagnetic radiation and stellar matter. Its strength depends on the momentum transfer per photon absorbed or scattered in the irradiated photosphere and is generally a very complicated function of local opacity and optical depth.

In the presence of a radiation source, the equation of hydrostatic equilibrium relating the pressure P, the density ρ, and the potential Φ for any point $\boldsymbol{r}(r,\theta,\phi)$ in the secondary, will acquire an additional term corresponding to the force due to this *external* radiation pressure,

$$\boldsymbol{\nabla} P = -\rho \boldsymbol{\nabla} \Phi + \frac{\kappa \rho}{c} f(\tau)\, \hat{\boldsymbol{n}}_1, \tag{1}$$

where $\hat{\boldsymbol{n}}_1$ is a unit vector in the direction of the external radiation, κ is the local opacity, c the speed of light, f the irradiation flux and τ the local optical depth in the secondary envelope with respect to the external radiation. (Here we have neglected inertial terms due to the rotation of the system, i.e. the Coriolis force and circulation terms.) For a given source luminosity, $f(\tau)$ at a point below the atmosphere will depend both on the local physical and chemical conditions in the secondary's envelope and on the geometry of the system, i.e. the distance from the radiation source and the angle of incidence of the flux vector. The complicated functional dependence of this term renders a precise analytical representation impossible. To obtain an explicit expression for this term, we generally make the simplifying assumption that the X-ray flux decreases exponentially (see e.g. Podsiadlowski 1991, 1992),

i.e.

$$f(\tau) \sim \frac{L_{\rm x}}{4\pi |\boldsymbol{r} - \boldsymbol{r}_1|^2}\, e^{-\tau}, \tag{2}$$

where $|\boldsymbol{r} - \boldsymbol{r}_1|$ represents the distance from the radiation source, and $L_{\rm x}$ denotes its X-ray luminosity.

However, in general the irradiation term in equation (1) does not represent a conservative force, i.e. a force that can be written as the gradient of a scalar potential, since it depends on the local conditions in the region of flux absorption. Therefore the inclusion of radiation pressure in the force equation precludes the existence of an equipotential surface. This also implies that there exists no surface for which the tangential force component is identical zero everywhere. An accurate determination of the irradiated secondary surface would therefore require a full treatment of the surface motion, including the meridional circulation of stellar material due to rotation (Von Zeipel 1924a) and the additional circulatory currents driven by the external radiation. A full solution is beyond the scope of this paper, and the correct circulation patterns even for non-irradiated single stars are still subject to debate (Osaki 1982; Charbonneau 1992; Maeder & Zahn 1998).

The purpose of this paper is to investigate the effects of the external irradiation in the absence of circulatory currents, i.e. we consider the extreme case in which tangential forces on the irradiated surface are small. In effect, we will seek a solution for which the irradiated surface locally approximates an equipotential surface. Compared to a solution that fully accounts for irradiation-driven circulation, one may expect that the true surface of an irradiated star will lie somewhere between this extreme case and the standard Roche potential.

3 A MODIFIED ROCHE POTENTIAL

Even though the surface of an irradiated star cannot be represented by an exact equipotential surface, one can still modify the classical Roche potential to account for the radiation-pressure term in an approximate way.

To to this, we first rewrite equation (1), expressing the

balance of forces per unit volume at the secondary surface, using the approximation of equation (2),

$$\begin{aligned}\boldsymbol{\nabla} P + \rho \boldsymbol{\nabla} \Phi_1 \quad &= \quad -\rho \frac{GM_1}{|\boldsymbol{r} - \boldsymbol{r}_1|^2}\, \hat{\boldsymbol{n}}_1 \\ &\quad + \frac{\kappa\rho}{c} \frac{L_{\rm x}}{4\pi |\boldsymbol{r} - \boldsymbol{r}_1|^2} e^{-\tau}\, \hat{\boldsymbol{n}}_1. \end{aligned} \tag{3}$$

Here the effective potential Φ_1 combines the gravitational potential of the secondary, treated as a point mass, with the non-inertial potential terms due to the rotation of the system (i.e. due to the centrifugal force).

Depending on the irradiation spectrum and the local physical and chemical conditions in the secondary, the external flux will penetrate to a certain depth below the photosphere. In our treatment of the irradiated surface, we will consider a layer of sufficient depth that most external radiation has been absorbed. However, this depth should be small compared to the secondary's radius, in order that $|\boldsymbol{r} - \boldsymbol{r}_1|$ can be considered constant in this region and κ and ρ can be well represented by average values $\bar{\kappa}$ and $\bar{\rho}$. Momentum transfer can then be regarded as an 'on the spot' event.

We now integrate equation (3) in the direction of the flux vector $\hat{\boldsymbol{n}}_1$, from the top of the secondary's atmosphere to some fixed surface layer of vertical optical depth $\tau_{0,n} \gg 1$. We denote the path length of penetration as s_0 with a corresponding optical depth to X-rays as $\tau_0 = \tau_{0,n} \sec\gamma$, where γ is the angle between the surface normal and the flux direction $\hat{\boldsymbol{n}}_1$. With the assumption that only the exponential term changes significantly over this distance, the right-hand side of equation (3) becomes

$$-\bar{\rho} \frac{GM_1}{|\boldsymbol{r} - \boldsymbol{r}_1|^2} \int_0^{s_0} {\rm d}s + \frac{\bar{\kappa}\bar{\rho}}{c} \frac{L_{\rm x}}{4\pi |\boldsymbol{r} - \boldsymbol{r}_1|^2} \int_0^{s_0} e^{-\tau} {\rm d}s. \tag{4}$$

The physical depth of penetration and the optical depth are related by ${\rm d}\tau = \bar{\kappa}\bar{\rho}\, {\rm d}s$ and therefore $\tau_0 = \bar{\kappa}\bar{\rho} s_0$. So for $\tau_0 \gg 1$, the right-hand side approximates to

$$\begin{aligned} &-\bar{\rho} \frac{GM_1}{|\boldsymbol{r} - \boldsymbol{r}_1|^2} s_0 + \frac{L_{\rm x}}{4\pi c |\boldsymbol{r} - \boldsymbol{r}_1|^2} \\ &\qquad = -\bar{\rho} \frac{GM_1}{|\boldsymbol{r} - \boldsymbol{r}_1|^2} s_0 \left\{ 1 - \frac{L_{\rm x}\bar{\kappa}}{4\pi G M_1 c \tau_0} \right\} \\ &\qquad = -\rho \frac{GM_1}{|\boldsymbol{r} - \boldsymbol{r}_1|^2} s_0 \left\{ 1 - \frac{f_t \bar{\kappa} \cos\gamma}{cg\tau_{0,n}} \right\}, \end{aligned} \tag{5}$$

where f_t is the total integrated flux and g the gravitational acceleration due to the compact radiation source. Since both of these quantities have the same $|\boldsymbol{r} - \boldsymbol{r}_1|$ dependence, the term in brackets in equation (5) is effectively constant for a given flux direction. Thus, at a given depth parallel to the top of the atmosphere, we may combine the forces due to gravity and radiation pressure from the compact object as a 'reduced' gravitational force

$$\boldsymbol{F}^{\rm eff}_{\rm grav} = \boldsymbol{F}_{\rm grav} - \boldsymbol{F}_{\rm rad} = (1-\delta)\boldsymbol{F}_{\rm grav}, \tag{6}$$

where $\delta = \text{constant} \times \cos\gamma$. The factor δ, expressing the ratio of radiation to gravitational forces, therefore depends only on the cosine of the angle between the surface normal and the flux vector. However, it is this dependence that renders the reduced force non-central.

We now extend the concept of a reduced force to define a reduced potential. Both gravitational and radiative forces due the X-ray source can then be characterised as $-(1-\delta)\int \boldsymbol{F}.{\rm d}\boldsymbol{r} = (1-\delta)\phi_{\rm grav}$, and the standard Roche expression for the binary potential may be modified directly by the inclusion of this $(1-\delta)$ factor. This formulation is strictly only valid in the case where gravitation and radiation pressure are acting in exactly opposite directions, and the resulting equipotential surface lies normal to both. The $\cos\gamma$ dependence of δ implies that this condition is not fulfilled, i.e. that a fictitious force results from the inclusion of a variable δ factor in the total potential (see § 4.1).

A number of authors have previously attempted to derive equipotential surfaces based on a reduced gravitational potential (e.g. Schuerman 1972; Kondo & McCluskey 1976; Vanbeveren 1977; Zhou & Leung 1988). However, these attempts did not fully account for the true physical and geometric conditions of irradiated systems, resulting in unrealistic solutions. We base our approach on the method developed by Drechsel et al. (1995), who treated the geometry in a far more sophisticated way, although we use a different treatment for the inner Lagrangian point and extend their model to include the effects of an accretion disc, if present.

4 DESCRIPTION OF THE MODEL

Following Drechsel et al. (1995), we use a modified Roche potential that approximately accounts for the effects of external irradiation to calculate the surface of the secondary, assumed to coincide with an equipotential surface. Since the external pressure force cannot be represented analytically, the equipotential surface must be calculated numerically. In the case of an accreting binary system, the model must also take into account the presence of an accretion disc, which may shadow a significant portion of the secondary and most importantly the inner Lagrangian (L_1) point. In addition, when applying these modified surfaces to the calculations of photometric lightcurves or radial velocity curves, the effects of gravity- and limb-darkening, which cause significant perturbations to the surface temperature distribution, must also be included. This also requires a precise numerical determination of the gradients of the potential on the stellar surface.

We consider the compact object as an isotropic point source of radiation, a fraction of which is incident on the surface of the secondary. The dimensionless ratio of radiation-pressure force to the gravitational force due to the compact companion at a given position on the secondary is defined as

$$\delta(r, \theta, \phi) = \frac{|\boldsymbol{F}_{\rm rad}|}{|\boldsymbol{F}_{\rm grav}|}. \tag{7}$$

In the case where the irradiation flux is totally absorbed in the secondary's surface layer, which will be largely justified in the case of irradiation by hard X-rays (see §4.4), these forces will be co-directional. We may then use the approximations of a reduced gravitational force and a reduced potential introduced in the previous section. We take the centre of the secondary star as the origin of spherical polar coordinates, with the compact object along the polar axis of the coordinate system (i.e. in the direction $\theta = 0$) and the pole of the secondary in the direction $\theta = 90^\circ, \phi = 0$. The value of delta varies as the angle γ between the surface normal and flux vector increases from its minimum value

obtained when the flux vector lies along the line of centres, up to 90° at the horizon, causing a respective decrease in the radiation-pressure force proportional to the $\cos\gamma$ term in equation (5).

In the Roche model, the stellar surfaces are obtained as closed equipotential surfaces for given values of the potential and mass ratios (Kopal 1959). When radiation pressure is included as a reduced gravitational potential, the modified total potential for a surface element of the secondary star, assuming synchronous rotation, takes the dimensionless form

$$\begin{aligned} -\Omega(r,\theta,\phi) &= \frac{1}{r} + q\frac{1-\delta(r,\theta,\phi)}{\sqrt{1-2\lambda r+r^2}} - q\lambda r \\ &\quad + \frac{(q+1)}{2}r^2(1-\nu^2), \end{aligned} \tag{8}$$

where $\lambda = \cos\theta$ and $\nu = \sin\theta\cos\phi$.

The variation of δ across the surface of the secondary has to be evaluated numerically. Once specified, the stellar surfaces can be determined point by point using a standard Newton-Raphson scheme (see e.g. Press et al. 1992). For given values of q and the critical potential Ω_0, the radius $r_0(\theta,\phi)$ for any direction (θ,ϕ) is obtained iteratively from the condition that the function g, defined as

$$g(\theta,\phi,r,\Omega_0,q) = \Omega_0 - \Omega(\theta,\phi,r,q), \tag{9}$$

is identical zero.

Writing $\delta = \delta_{\max}\cos\gamma$, we may relate $\delta_{\max}$ to the stellar mass and luminosity of the companion, and to the mean absorption coefficient $\bar{\kappa}$ (see equ. 5). This will generally be a complicated function, varying significantly across the surface of the secondary. In the present, exploratory investigation, we shall therefore make the simplifying assumption that $\delta_{\max}$ can be treated as an independent parameter. This has the added advantage of only introducing one new parameter into the expression for the modified potential. This is desirable given the already large number of parameters necessary to specify the physical and geometrical structure of close binaries even for the classical Roche model. In §4.4, we shall make some rough estimates of the magnitude of $\delta_{\max}$ for typical parameters found in X-ray binaries

4.1 Validity of the model

Before we proceed to apply this model, we need to discuss its limitations. As already stressed in §2, the external radiation pressure force is not a conservative force and thus cannot be expressed precisely as the gradient of a potential. By assuming that the surface of the secondary coincides with one of these modified equipotential surfaces, we therefore make an error in the force equation (equ. 1) by effectively introducing a fictitious force. In addition, the assumption of hydrostatic equilibrium ignores the effects of irradiation-driven circulation.

4.1.1 The fictitious force

In our formulation, the external radiation pressure force is introduced as a reduction in the gravity term, $(1-\delta)\boldsymbol{F}_{\rm grav}$ (as in equ. 6). The modified potential due to the combined forces of radiation and gravity from the compact object is then taken to be $-(1-\delta)\int \boldsymbol{F}.\mathrm{d}\boldsymbol{r}$, as in the second term of equation (8). However, this clearly introduces a fictitious and unphysical force due to the variation of δ given by

$$\boldsymbol{F}_\delta = -\frac{\partial\Omega}{\partial\delta}\boldsymbol{\nabla}\delta. \tag{10}$$

In order to see the effect of this term on the determination of the surface geometry, it is helpful to visualize that the construction of the equipotential surface is equivalent to piecing together surface elements that are perpendicular to the net local force. This provides a unique solution as long as there are a sufficient number of boundary conditions that allow a complete covering of the surface by these surface elements. In the present problem this is easily fulfilled since many surface points are already fixed, irrespective of irradiation – for example, those in the shadowed region, once the potential at the inner Lagrangian point is specified. The forces derived from the modified potential then provide a good representation of the actual forces if, for all points, the fictitious force component does not significantly perturb the surface normal vector parallel to the actual force, $-(\boldsymbol{\nabla}\Omega)_\delta$, given by the gradient of the potential with δ kept constant.

To quantify this condition, we define the 'true' irradiated surface by the constraint

$$-(\boldsymbol{\nabla}\Omega)_\delta \wedge \hat{\boldsymbol{n}}_0 = 0, \tag{11}$$

where $\hat{\boldsymbol{n}}_0$ is the unit vector normal to the surface. By using a reduced potential, as given by equation (8), the surface actually calculated is given by

$$[-(\boldsymbol{\nabla}\Omega)_\delta + \boldsymbol{F}_\delta] \wedge [\hat{\boldsymbol{n}}_0 + \delta\hat{\boldsymbol{n}}_0] = 0. \tag{12}$$

The quantity $\delta\hat{\boldsymbol{n}}_0$ represents the deviation from the true surface normal and hence should be small ($\ll 1$) for the model to represent the surface geometry faithfully. Expanding this expression and using equation (11), we obtain

$$[-(\boldsymbol{\nabla}\Omega)_\delta \wedge \delta\hat{\boldsymbol{n}}_0] + [\boldsymbol{F}_\delta \wedge \hat{\boldsymbol{n}}_1] = 0, \tag{13}$$

where $\hat{\boldsymbol{n}}_1 = \hat{\boldsymbol{n}}_0 + \delta\hat{\boldsymbol{n}}_0$ is the calculated surface normal in the model. But $-(\boldsymbol{\nabla}\Omega)_\delta \equiv |(\boldsymbol{\nabla}\Omega)_\delta|\hat{\boldsymbol{n}}_0$, and hence we may write

$$|\hat{\boldsymbol{n}}_0 \wedge \delta\hat{\boldsymbol{n}}_0| = \frac{|\boldsymbol{F}_\delta \wedge \hat{\boldsymbol{n}}_1|}{|(\boldsymbol{\nabla}\Omega)_\delta|}. \tag{14}$$

It follows from the definition of a unit vector that $|\hat{\boldsymbol{n}}_0 \wedge \delta\hat{\boldsymbol{n}}_0| \approx |\delta\hat{\boldsymbol{n}}_0|$ (correct to second order in $\delta\hat{\boldsymbol{n}}_0$). Thus, the requirement that $|\delta\hat{\boldsymbol{n}}_0| \ll 1$ may be expressed as

$$\eta \equiv \frac{|\boldsymbol{F}_\delta \wedge \hat{\boldsymbol{n}}|}{|(\boldsymbol{\nabla}\Omega)_\delta|} \ll 1. \tag{15}$$

When this inequality is satisfied, the inclusion of the effects of external radiation pressure in the form of a modified potential only introduces a small error in the determination of the surface geometry.

4.1.2 The role of circulation

In our present model we do not consider the effects of irradiation-induced circulation in the outer layers of the secondary (see e.g. Kippenhahn & Thomas 1979). Indeed, in general there is no physical reason why the surface of the secondary should be an equipotential surface, even approximately, if circulation terms are important. If a Roche-lobe filling secondary is suddenly being irradiated, its surface

would not immediately (i.e. on a dynamical timescale) adjust to one of our modified equipotential surfaces, since the pressure inside the star, a few pressure scale heights below the surface, is always much larger than the external irradiation pressure. Instead, the main effect of a sudden turn-on of the external irradiation is to drive circulation that would move matter in the surface layer away from the irradiated side. However, this circulation can only be maintained as long as matter is resupplied from below. This will generally not be possible for an arbitrary surface geometry. Hence the surface will readjust until a closed steady-state circulation system is established (note, however, that even the existence of a steady state is by no means guaranteed). This demonstrates that, for a realistic treatment, the surface geometry of an irradiated secondary has to be determined simultaneously with the circulation. The inclusion of circulation is beyond the scope of the present paper, but we have already initiated a detailed study of its consequences. By assuming that the surface is given by a modified equipotential, we effectively minimize the effects of circulation. In this sense, these surfaces represent an extreme limit, and we may expect that the true surface of an irradiated secondary lies somewhere between this limit and the other extreme, the unperturbed Roche potential.

4.2 Evaluation of $\delta(r, \theta, \phi)$

In our calculations we divide the surface of the secondary into an array of grid points spaced equally in θ and ϕ. The value of $\delta(r, \theta, \phi)$ is then determined for all grid points, where we need to take into account shadowing by an accretion disc, if present. In all cases, we assume that the compact object is a point source of radiation.

4.2.1 Systems without accretion discs

In systems without an accretion disc, there is no shielding of the secondary, and δ has its maximum value along the line of centres, at the point $\theta = \phi = 0$. At all other points, δ is calculated according to

$$\delta(r, \theta, \phi) = \begin{cases} \delta_{\max} \cos\gamma(r, \theta, \phi) & \text{if } \cos\gamma > 0 \\ 0 & \text{otherwise,} \end{cases} \tag{16}$$

where $\gamma(r, \theta, \phi)$ is the angle subtended by the surface normal and the vector directed from the point (r, θ, ϕ) to the source of the radiation. The constant $\delta_{\max}$ is an input parameter, which defines the maximum value of δ obtained in the absence of an accretion disc when the flux vector is incident normally on the irradiated surface. (Note, however, that there may not be any region of the surface on which the flux vector is incident normally; see §5.1.1.)

4.2.2 Systems with Accretion Discs

Low-mass X-ray binaries (LMXBs) in general and many high-mass X-ray binaries (HMXB) are believed to contain some form of an accretion disc. A disc will cast a shadow on a significant portion of the secondary's surface and will generally shield the L_1 point from external irradiation.

To model the effect of this shadowing, we assume that the accretion disc is axially symmetric and has an inner opaque region and an outer region which transforms smoothly from opaque to transparent at the outermost edge.

We define the opening (half) angle of the disc as α and assume that the disc is completely opaque within an angle β_1 of the equatorial plane ($\beta_1 < \alpha$), where these angles are defined with respect to the compact object.

In Cartesian coordinates, where the compact object lies along the x-axis and where the axis of orbital rotation and the axis of symmetry of the accretion disc are parallel to the z-axis, β is given by

$$\sin\beta = |z|/d, \tag{17}$$

where d denotes the distance from a point on the secondary (x, y, z) to the compact object, given by

$$d = ((a - x)^2 + y^2 + z^2)^{1/2} \tag{18}$$

and where a is the orbital separation.

To model the partially transparent region of the disc, we define a composite function $T(r, \theta, \phi)$:

$$T = \begin{cases} 0 & \text{if } \beta \le \beta_1 \\ \frac{1}{2}\left\{1 - \cos\left[\left(\frac{\beta - \beta_1}{\alpha - \beta_1}\right)\pi\right]\right\} & \text{if } \beta_1 \le \beta \le \alpha \\ 1 & \text{if } \beta \ge \alpha. \end{cases} \tag{19}$$

We also tested a linear transparency function in the partially transparent region, but found that a smooth sinusoidal dependence improves the rate of convergence in the numerical iteration process.

Using this penetration factor, values of $\delta(r, \theta, \phi)$ are determined over the surface of the secondary in a similar manner to equation (16),

$$\delta(r, \theta, \phi) = \begin{cases} \delta_{\max} T \cos\gamma(r, \theta, \phi) & \text{if } \cos\gamma > 0 \\ 0 & \text{otherwise,} \end{cases} \tag{20}$$

where the constant $\delta_{\max}$ is defined as before.

4.3 The convergence procedure

We now have a recipe for calculating $\delta(r, \theta, \phi)$ in terms of $\gamma(r, \theta, \phi)$ over the surface of the secondary. The angle $\gamma(r, \theta, \phi)$ is the angle subtended by the surface normal and the vector from the point (r, θ, ϕ) to the radiation source. Its evaluation requires the knowledge of the 3-dimensional surface of the secondary under the influence of radiation pressure, which is *a priori* unknown and can only be determined iteratively.

Following Drechsel et al. (1995), we model the surface of the secondary in the first iteration as a triaxial ellipsoid, defined by

$$\frac{x^2}{r_{\text{point}}^2} + \frac{y^2}{r_{\text{side}}^2} + \frac{z^2}{r_{\text{pole}}^2} = 1, \tag{21}$$

with semi-axes r_{point}, r_{side}, and r_{pole} identical with the Roche radii in the directions $(\theta = 0)$, $(\theta = 90^\circ, \phi = 90^\circ)$, and $(\theta = 90^\circ, \phi = 0)$, respectively. The radii r_{side} and r_{pole} are taken to be equal to the classical Roche radii since these points lie beyond the radiation horizon. In the presence of an accretion disc, we assume that the inner Lagrangian point is shielded from radiation – hence r_{point} will also be equal to the classical Roche radius. In systems which do not contain a disc, the position of the L_1 point will be modified. The

value of δ at this point must simultaneously satisfy the requirement that the total force along the x-axis vanishes, i.e. $\partial\Omega/\partial x = 0$ (where Ω is given by equation 8), and must also satisfy equation (16), which relates δ to the surface normal. Note that, as in the case of the unperturbed Roche lobe, the surface normal at the L_1 point is strictly undefined. We therefore consider a point infinitesimally close to the L_1 point and obtain an approximate surface normal by extrapolation. The value of $r_{\rm point}$ is then fixed and forms one boundary condition for the iteration scheme.

In each iteration, we need the vector from each surface grid point to the radiation source and the vector defining the surface normal. The former is readily calculated. However, a correct calculation of the surface normal is a crucial factor for a numerically stable iteration process, since this affects the variation of δ with θ over the irradiated region. For a correctly converging solution, δ must fall to zero *continuously* (though not necessarily smoothly) at the interface points, i.e. those points which separate the irradiated and shadowed regions. This forms a second boundary condition. We also require a continuous variation of δ over the region shadowed by the accretion disc (this is ensured by our choice of the functional form of the transparency function in equ. 19).

Thus, for any point on the irradiated ellipsoid, the surface normal and flux vectors are determined. A value for γ can then be calculated and hence the local value of δ. Substituting these δ values into the modified potential equation (8) then allows the determination of improved radius values for all points on the surface by application of the Newton-Raphson scheme.

4.4 Physical estimates of $\delta_{\rm max}$

So far we have considered $\delta_{\rm max}$ as a free parameter. However, it is straightforward to estimate the value of $\delta_{\rm max}$ for actual binary systems.

Consider an irradiated secondary. The radiation pressure acting on a unit surface element of the secondary is given by

$$P_{\rm rad} = \frac{1}{c}\int_{\omega}\int_{\nu} I_\nu \cos^2\gamma \,{\rm d}\nu\,{\rm d}\omega, \tag{22}$$

where c is the velocity of light, γ is the angle between the surface normal and the incident radiation, ${\rm d}\omega$ is the opening solid angle of the radiation cone, and I_ν the intensity in the frequency interval ${\rm d}\nu$ around ν. Assuming a plane parallel atmosphere and negligible scattering of the incident radiation, we obtain for the radiation force per unit mass

$$F_{\rm rad} = -\frac{1}{\rho}\frac{{\rm d}P_{\rm rad}}{{\rm d}r} = \frac{1}{c}\int_{\omega}\int_{\nu} \kappa_\nu I_\nu \cos^2\gamma \,{\rm d}\nu\,{\rm d}\omega, \tag{23}$$

where ρ is the mass density and κ_ν the monochromatic absorption coefficient for radiation absorbed by the secondary. By taking an integrated mean opacity, $\bar{\kappa}$, we may take this quantity out of the integral and obtain $F_{\rm rad} = f_t\bar{\kappa}/c$, where f_t is the total integrated flux. The gravitational force due to the compact object per unit mass of the secondary is simply $F_{\rm grav} = GM/d^2 = g$, where M and d are the mass of the compact object and its distance from a point on the irradiated component. The maximum ratio of pressure to gravitational forces, assuming normally incident radiation ($\gamma = 0$), is therefore given by

$$\delta_{\rm max} = \frac{F_{\rm rad}}{F_{\rm grav}} = \frac{f_t\bar{\kappa}}{cg}, \tag{24}$$

which has the same functional dependence as in equation (5). We may also relate $\delta_{\rm max}$ to the Eddington luminosity of the secondary, $L_{\rm Edd}$. Writing the flux as $f_t = L/4\pi d^2$, where L is the irradiating luminosity, $\delta_{\rm max}$ becomes

$$\delta_{\rm max} = \frac{L\bar{\kappa}}{4\pi d^2 cg} = \frac{L\bar{\kappa}}{4\pi cGM} = \frac{1}{q}\frac{L}{L_{\rm Edd}}, \tag{25}$$

where m is the mass of the secondary, and $q = M/m$ is the mass ratio.

In general, for a given frequency of radiation, the opacity will be a very sensitive function of the local temperature, density and chemical composition, and can vary by orders of magnitude across the surface of the secondary. If the material on the surface of the secondary consisted of fully ionized hydrogen, electron scattering would be the dominant opacity source, i.e. $\bar{\kappa} = \sigma_{\rm T}/m_{\rm p} \sim 0.4$ cm^2 g^{-1}, where $\sigma_{\rm T} = 6.7\times10^{-25}$ is the Thomson cross section.

For systems where the luminosity in X-rays is close to the Eddington luminosity or where $\bar{\kappa}$ is much larger than the Thomson opacity, the ratio of radiative to gravitational forces may easily be of order unity, implying a significant deformation of the classical Roche lobe. Indeed, it is possible that $\delta_{\rm max}$ exceeds unity. In this case, there would be no inner Lagrangian point. However, this is unlikely in practise as such systems are very likely to contain a thick accretion disc which will shield much of the inner face of the secondary.

5 THE EFFECTS OF EXTERNAL RADIATION PRESSURE ON THE BINARY STRUCTURE

External radiation pressure changes the structure and appearance of the secondary compared to the case of Roche-lobe overflow without irradiation; the most important effects are: (1) the distortion of the secondary's surface, and the associated change in the surface temperature distribution which affects the modelling of lightcurves and radial velocity curves (see § 6); and (2) a possible change of the critical configuration for systems which do not contain accretion discs (or contain discs which are tilted with respect to the binary plane), where the L_1 point is directly irradiated, which affects mass transfer and mass loss from the system. We will discuss these various possibilities in detail in this and the subsequent section.

5.1 The binary configuration

Let us first consider the effects of radiation pressure in systems without accretion discs. This case has possible applications to binary pulsar systems, stars orbiting supermassive black holes and, in some cases, high-mass X-ray binaries.

To illustrate how external irradiation can change the binary configuration, we considered a binary with a fixed mass ratio $q = M_1/M_2 = 2$, but with different values for $\delta_{\rm max} = 0.0$, 0.15, 0.30 and 0.50 and calculated the critical modified potential, as described above, such that the secondary fills its maximum possible volume. In Figure 1 we present meridional sections in the x-z plane of the modified critical potential surfaces for this sequence of models, where the same scale has been used in all panels.

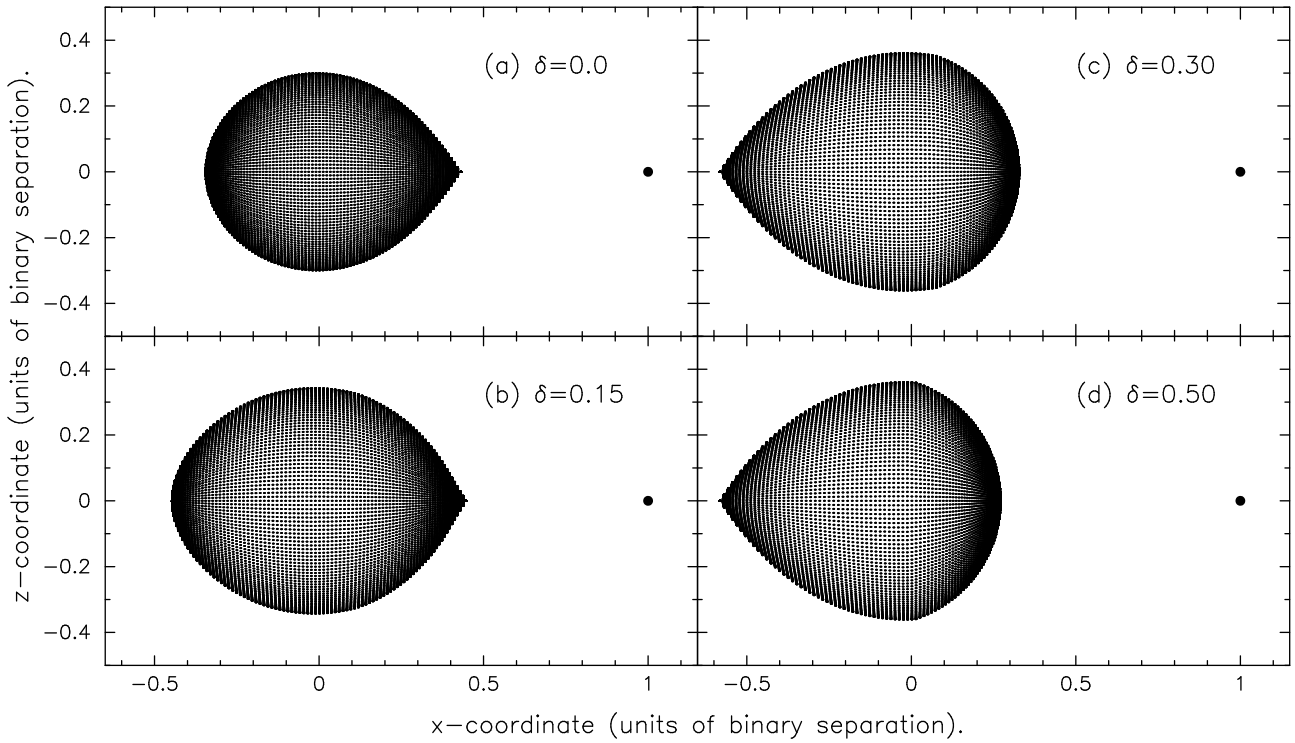

Figure 1. A sequence of modified 'Roche' lobes including the effects of external irradiation for a binary system with mass ratio $q = M_1/M_2 = 2$. The compact companion, of mass M_1, is represented as a single point at coordinates (1,0). The values of $\delta_{\max}$, the maximum ratio of the external radiation force to the gravitational force due to the compact star at the secondary surface, are set to (a) 0.0 (the standard Roche lobe), (b) 0.15, (c) 0.30, and (d) 0.50, respectively.

Figure 1a shows the unperturbed Roche lobe without external irradiation pressure. In Figure 1b the external irradiation force has been increased to 15 per cent of the gravitational force. As a consequence, the modified inner Lagrangian point L_1 moves towards the compact object (since its effective gravity has been reduced), and the volume of the critical potential lobe increases. The critical potential, as defined by equation (8), decreases in magnitude as δ is increased, until it reaches the same value as the potential of the outer Langrangian point, L_2, which is unaffected by irradiation as it always lies in the shadowed region of the secondary. Once the outer Lagrangian point has a higher potential than the inner Lagrangian point, it takes over the role of defining the potential of the critical lobe, and the critical potential then passes through L_2 rather than L_1. This change from an inner to an outer critical configuration implies that mass loss now takes place through the outer rather than the inner critical point, most likely leading to the formation of a circumbinary disc and mass loss from the system rather than mass transfer to the compact object. For $q = 2$, this transition occurs at $\delta_{\max} = 0.202$. In Figure 1c, where $\delta_{\max} = 0.30$, the switch of configuration has already occurred. Increasing δ further no longer changes the position of L_2 (since its potential is unaffected by external radiation), but the shape of the critical potential is further deformed and its enclosed volume decreases (see Figure 1d).

5.1.1 The conical inner Lagrangian point

As can be seen if Figure 1, for $\delta_{\max} < \delta_{\rm crit}$, where $\delta_{\rm crit}$ is the critical value at which the system configuration change occurs, the region around the irradiated L_1 point has a conical geometry (as for the standard Roche lobe). Hence the normal vector at the L_1 point is undefined, and its position must be determined from the asymptotic value obtained in its neighbourhood (i.e. in the limit of small θ, the angle measured from the line-of-centres, or x-axis). Because of the centrifugal term in the total potential (equ. 8) there is no axial symmetry about the x-axis. The asymptotic value of the L_1 normal vector therefore depends on the plane containing the x-axis being considered, i.e. it depends on the angle ϕ. The *critical* equipotential surface is defined as the surface with the lowest potential for which any matter can leave the secondary's gravitational field. It is easy to show that this is the case for $\phi = 0$; this implies that an expanding irradiated secondary star will first lose mass through the inner Lagrangian point in the x-z plane. (In practice however, if mass loss takes place, the overflowing material is likely to be optically thick and will therefore shield the L_1 point from radiation, thus obscuring the subtle geometrical details described above.)

The conical nature of the irradiated L_1 point also implies that the maximum value of the ratio δ, obtained by extrapolation, is less than $\delta_{\max}$. At no point on the irradiated stellar surface is the flux vector at normal incidence. This is in contrast to the model described by Drechsel et al. (1995) in which the L_1 point is apparently calculated assuming perpendicular incidence of the external radiation

flux, such that $\delta = \delta_{\rm max}$ at this point. Such a 'flat' L_1 point also affects the critical value, $\delta_{\rm crit}$, at which the configuration change occurs. In the Drechsel model it is lower for a given mass ratio q. For example, for $q = 2$ it would occur at $\delta_{\rm crit} = 0.167$ for the assumption of a flat L_1 point instead of $\delta_{\rm crit} = 0.202$, as obtained above.

To show that a flat geometry near the L_1 point is not appropriate, one can examine the factor η defined in §4.1.1 (see equ. 15), which compares the fictitious force acting within the equipotential surface (resulting from the equipotential approximation) to the 'true' force directed approximately normally to this surface. We find that η is at least an order of magnitude less than $\delta_{\rm max}$ at all points; this confirms that this modified equipotential surface provides a good representation of the 'true' forces. On the other hand, for a flat L_1 geometry, η is always of order unity in the neighbourhood of the L_1 point. This implies that the true and fictitious forces are of comparable magnitude and proves that the corresponding equipotential surface provides a poor approximation for an irradiated surface.

(Note that both models are consistent for outer critical configurations set by the L_2 potential. In this case, the irradiated surface at $\theta = 0$ is flat and δ acquires its maximum value at this point, $\delta_{\rm max}$.)

5.2 Implications for binary pulsar systems

As shown in § 5.1, if the irradiation force exceeds a critical value of the gravitational force, $\delta_{\rm max}$, the critical potential configuration changes from an inner to an outer configuration. However, this can only apply to systems in which the inner Lagrangian point is directly irradiated and hence can never be the case for systems like low-mass X-ray binaries where the accretion disc effectively screens the L_1 point from the X-ray irradiation. In such systems, the main consequence of irradiation will be a deformation of the surface (see § 6).

On the other hand, binary systems containing millisecond pulsars probably do not contain accretion discs. Hence pulsar radiation (in the form of electromagnetic waves, particle flux, etc.) can play the role of X-rays and can potentially cause a configuration change. Mass will then be lost from the outer Lagrangian point, which may then leave the system entirely. Continued irradiation may eventually lead to the total evaporation of the secondary. This is the main mechanism, originally proposed by Ruderman, Shaham & Tavani (1989), by which pulsars may be able to destroy their companions leaving a single millisecond pulsar. The "black-widow" pulsar, PSR 1957+20 (Fruchter et al. 1988), and the binary pulsar PSR 1718+19 (Lyne et al. 1990; McCormick & Frank 1993) are believed to be examples where the pulsar radiation is in the process of evaporating the companion.

In the case of PSR 1957+20, the mass function and the radio eclipse suggest a secondary mass near $0.022\,{\rm M}_\odot$ (for an assumed pulsar mass of $1.4 M_\odot$; e.g. Fruchter et al. 1988). This implies a mass ratio of around 60 and a corresponding value for $\delta_{\rm crit}$ of approximately 0.01 (see Table 1). One can also estimate the pulsar luminosity from the observed spin-down rate to be $\sim 40\,L_\odot$ (e.g. Fruchter et al. 1990). For the irradiated component we have $L_{\rm Edd} \simeq (10^{36}\,\bar\kappa^{-1})\,{\rm erg\,s^{-1}}$, and therefore $\delta_{\rm max} = L/qL_{\rm Edd} = 0.0025\,\bar\kappa$. So $\delta_{\rm max}$ will exceed $\delta_{\rm crit}$ if the mean photospheric opacity on the irradiated side is greater than ~ 4 cm^2 g^{-1}, a value that may not be unreasonable (it depends on the uncertain thermodynamic parameters in the irradiated photosphere of the secondary). In this case, we may expect a configuration change where mass loss occurs from the outer Lagrangian point, leading to the formation of an excretion disc rather than an accretion disc.

[t]

Table 1. Values of $\delta_{\rm crit}$, the product $q\delta_{\rm crit}$, and $\Omega_{\rm crit}$ for a sequence of mass ratios

Mass Ratio, q	$\delta_{\rm crit}$	$q\delta_{\rm crit}$	$-\Omega_{\rm crit}$
0.5	0.459	0.230	2.408
1.0	0.318	0.318	3.207
1.5	0.246	0.369	3.949
2.0	0.202	0.405	4.655
2.5	0.172	0.431	5.335
10	0.0564	0.564	14.44
10^2	6.89E-3	0.589	109.7
10^3	7.48E-4	0.748	1.02E+3
10^4	7.76E-5	0.776	1.00E+4
10^5	7.89E-6	0.789	1.00E+5
10^6	7.94E-7	0.794	1.00E+6

5.3 Application to binary systems with extreme mass ratios

Table 1 shows the values of $\delta_{\rm crit}$, the product $q\delta_{\rm crit}$, and the critical potential $\Omega_{\rm crit}$ of the secondary, as defined by equation (8), for a sequence of mass ratios. For higher mass ratios, the critical value of $\delta_{\rm max}$ decreases, and the magnitude of the critical potential increases, corresponding to a smaller Roche volume. Note that the product $q\delta_{\rm crit}$ converges towards a constant value for increasing q. In conjunction with equation (25), this implies that in the asymptotic limit of high mass ratio, the critical luminosity scales directly with the Eddington luminosity of the irradiated object,

$$\begin{aligned} L_{\rm crit} &= q\delta_{\rm crit} L_{\rm Edd} \\ &\propto L_{\rm Edd}, \qquad \text{for } q \gg 1. \end{aligned} \tag{26}$$

A related formula was derived by Podsiadlowski & Rees (1994), where they expressed the difference in potential between the inner and outer Lagrangian points in terms of the ratio of irradiating to Eddington luminosities. Their equation (7) (without a spurious factor of $(m/3M)^{1/3}$) reads

$$\Delta U \equiv U_2 - U_1 \simeq \frac{Gm}{a}\left[\frac{2}{3} - \gamma\right], \tag{27}$$

where $\gamma = L/L_{\rm Edd}$, a is the binary separation, and m the mass of the irradiated star. However, this equation contains the assumption that the irradiating flux is perpendicular to the irradiated surface at L_1, i.e. $\delta_{\rm max}/\delta_{L_1} = 1$. As we have shown above, this is not a good approximation. Based on our calculations, performed for a range of values of q and $\delta_{\rm max}$, we find this ratio to be approximately 1.20. Hence the Lagrangian points have the same potential, i.e. $\Delta U = 0$, for $\gamma = 1.20 \times \frac{2}{3}$. Equation (26) therefore becomes

$$L_{\rm crit} \to 0.80 L_{\rm Edd}, \qquad \text{as } q \to \infty, \tag{28}$$

in agreement with table 1.

One interesting application of this case are low-mass stars orbiting supermassive black holes in active galactic nuclei (AGN) which are being irradiated by the central black hole. Such systems can be considered binaries with extreme mass ratios, typically of order 10^5 to 10^8, and some highly unusual properties (see e.g. Podsiadlowski & Rees 1994).

There is a general current consensus that AGN are powered by the accretion of matter onto the central black hole (see e.g. the reviews by Rees 1984; Frank, King & Raine 1992). Perhaps the strongest evidence for this picture derives from studies of X-ray emission, in which the combination of large luminosity (typically $\sim 10\%$ of the bolometric luminosity) and rapid variability imply an efficient energy generation mechanism confined within a small region (e.g. Fabian 1992). Although accretion is the most plausible explanation, it is not clear what the source of the fuel is. Tidal disruption of stars is one possibility or even Roche-lobe overflow of a star that spirals towards the black hole due to angular momentum loss caused by gravitational radiation (see Podsiadlowski & Rees 1994 for discussion and further references).

However, the X-ray luminosity in these systems will generally be far in excess of the Eddington luminosity of the stellar companion, $\sim 10^{38}$ erg s^{-1} for a star of order $1\,\mathrm{M}_\odot$. (In general, for luminous supermassive black holes, we may expect $L/L_{\mathrm{Edd}}^{\mathrm{star}} \sim 10^4$–$10^7$). So it is clear from equation (28) that only a tiny fraction of the central source's X-ray luminosity has to be emitted in the direction of the companion and reach the inner Lagrangian point for L to exceed L_{crit}. Hence any Roche-lobe overflow from the stellar companion must occur via the outer Lagrangian (L_2) point, leading to the formation of an excretion disc rather than an accretion disc. The tidal coupling between this excretion disc and the secondary may then provide a tidal barrier and actually prevent accretion of disc material onto the black hole (e.g. Artymowicz et al. 1991).

5.4 Self-sustaining mass loss through the outer Lagrangian point

In the previous sections, we showed how external irradiation pressure can change the configuration of the critical tidal lobe for the mass-losing component in a binary system from an inner to an outer critical configuration where mass loss occurs through the outer rather than the inner Lagrangian point. Since this matter will carry off an associated amount of angular momentum that is larger than the systemic specific angular momentum, this leads to a net decrease in the specific angular momentum of the system. Such mass loss can dramatically increase the mass-loss rate from the mass loser and sometimes even destabilize such systems completely. To estimate this more quantitatively, we give a simple analysis following along standard lines (see e.g. Rappaport, Verbunt & Joss 1983).

We consider a binary system whose components have masses M_1 and M_2, and circular Keplerian orbits of radius a_1 and a_2, with a total separation a. The system has an orbital period P, and the total orbital angular momentum of such a configuration is given by

$$J = \sqrt{\frac{Ga}{M_1 + M_2}}\, M_1 M_2. \tag{29}$$

Now suppose that the secondary loses mass by an amount δM_2, a fraction β of which is accreted by the primary while the remaining fraction leaves the system. In units of the orbital angular momentum of the secondary, the angular momentum lost from the system is therefore

$$\delta J = \alpha(1-\beta)\,\delta M_2\, a_2^2\, \frac{2\pi}{P}, \tag{30}$$

where the factor α depends on the details of the mass-loss mechanism. Using Kepler's Law and the relation $a_2 = M_1 a/(M_1 + M_2)$, we can combine equations (29) and (30) to obtain

$$\frac{\delta J}{J} = \alpha(1-\beta)\,\frac{\delta M_2}{M_2}\,\frac{M_1}{M_1 + M_2}. \tag{31}$$

Taking the logarithm of equation (29) and differentiating it with respect to M_2, and then equating the result with equation (31), we get

$$\frac{\delta \ln a}{\delta \ln M_2} = (1-\beta)\frac{2\alpha M_1 + M_2}{M_1 + M_2} + 2\,\beta\frac{M_2}{M_1} - 2. \tag{32}$$

Since the orbital separation changes because of the mass loss, the critical tidal lobe will adjust accordingly. Writing the effective radius of the critical tidal lobe as

$$\bar{R}_L = a\,\bar{f}(q), \tag{33}$$

where $q = M_1/M_2$ is the mass ratio and the function $\bar{f}$ depends on the exact shape of the critical lobe (for the standard Roche lobe, see the approximation by Eggleton [1983]). Even in the case of the irradiation-modified critical lobe we can factorize $\bar{R}_L$ in this form as long as the geometry of the modified potential remains self-similar (for a constant irradiation luminosity).

As mass is lost through the outer Lagrangian point, the separation will generally shrink and so will the critical lobe. If the critical radius decreases more rapidly than the thermal equilibrium radius of the secondary, the latter will no longer be able to remain in thermal equilibrium, and mass transfer will then be self-sustaining, i.e. be driven by the thermal expansion of the secondary or, in the most extreme case, occur on a dynamical timescale (see e.g. Ritter 1996 for a detailed review). This condition is best expressed in terms of the mass-radius exponent of the critical lobe and the equilibrium radius as

$$\xi_{\mathrm{L}} > \xi_{\mathrm{eq}},, \tag{34}$$

where

$$\xi_{\mathrm{L}} = \left(\frac{\mathrm{d}\ln R}{\mathrm{d}\ln M}\right)_{\mathrm{L}}, \text{ and } \xi_{\mathrm{eq}} = \left(\frac{\mathrm{d}\ln R}{\mathrm{d}\ln M}\right)_{\mathrm{eq}} \tag{35}$$

define the mass-radius exponents for the critical tidal lobe and stars in thermal equilibrium, respectively. Using equations (32) to (35), we then obtain

$$\xi_{\mathrm{L}} = -2 + (1-\beta)\frac{2\alpha q + 1}{q+1} + \frac{2\beta}{q} + \frac{d\ln\bar{f}}{d\ln q}\left(-1 - \frac{\beta}{q}\right). \tag{36}$$

Assuming now that all the mass is lost through the outer Lagrangian point and none is accreted by the compact object, and that this matter carries off exactly the specific angular momentum at the outer Lagrangian point, located at x-coordinate x_{L_2}, we can set $\beta = 0$ and obtain α from

$$\alpha = \frac{(|x_{L_2}| + a_2)^2}{a_2^2} = \left[\left(1 + \frac{1}{q}\right)\frac{|x_{L_2}|}{a} + 1\right]^2, \quad (37)$$

where $a_2 = M_1 a/(M_1 + M_2)$. Equation (36) then simplifies to become

$$\xi_{\rm L} = -2 + \frac{2\alpha q + 1}{q + 1} - \frac{{\rm d}\ln \bar{f}}{{\rm d}\ln q}. \quad (38)$$

The function ${\rm d}\ln \bar{f}/{\rm d}\ln q$ is generally a slowly varying function which will depend on the irradiation luminosity. In the case of the standard Roche formula (Eggleton 1983), it is easy to show that $\xi_{\rm L}$ is $\gtrsim 1$ for $q \lesssim 100$. Since $\xi_{\rm eq}$ is generally less than 1, this suggests that mass loss will generally be self-sustaining for $q \lesssim 100$, occurring either on a thermal or a dynamical timescale, if mass loss occurs through the outer Lagrangian point. For comparison, in the case of conservative mass transfer through the inner Lagrangian point, the condition $\xi_{\rm L} \simeq 1$ corresponds to a mass ratio $q \simeq 0.8$.

The change of the orbital separation is related to a change in orbital period by Kepler's Third Law which can be written in its differentiated form as

$$\frac{\dot{P}}{P} = \frac{3}{2}\frac{\dot{a}}{a} - \frac{(1-\beta)\dot{M}_2}{2(M_1 + M_2)}. \quad (39)$$

Combining this with equation (32), we obtain

$$\frac{\dot{P}_{\rm orb}}{P_{\rm orb}} = 3f\frac{\dot{M}_2}{M_2}, \quad (40)$$

where

$$f = \frac{\beta}{q} - \left\{\frac{2/3 + \beta/3 + q\,[1 - \alpha(1-\beta)]}{1+q}\right\}. \quad (41)$$

(This treatment does not include any tidal interaction terms due to a difference in rotational and orbital angular frequencies.) In the case of non-conservative mass loss through the L_2 point ($\beta = 0$), this reduces to

$$\frac{\dot{P}_{\rm orb}}{P_{\rm orb}} = -\left\{\frac{2 + 3q\,(1-\alpha)}{1+q}\right\}\frac{\dot{M}_2}{M_2}, \quad (42)$$

relating the period change to the mass-loss rate from the secondary.

In recent years, a number of systems have been observed to exhibit orbital period decays, for example, the massive X-ray binary SMC X-1 with $\dot{P}_{\rm orb}/P_{\rm orb} = (-3.36 \pm 0.02) \times 10^{-6}$ yr^{-1} (Levine et al. 1993) and the system Centaurus X-3 with $\dot{P}_{\rm orb}/P_{\rm orb} = (-1.8 \pm 0.1) \times 10^{-6}$ yr^{-1} (Kelley et al. 1983). These period changes have traditionally been explained by a tidal instability, the Darwin instability, which causes the orbit to decay in the process of spinning up the secondary (Darwin 1879; Pringle 1974).

However, as we shall demonstrate below, using Cen X-3 as an example, a relatively moderate outflow through L_2 could also account for the observed change and may help explain some other observations that are not well understood at the present time.

5.5 Application to Centaurus X-3

Centaurus X-3 is a massive X-ray binary with an orbital period of 2.87 d, observed to radiate near the Eddington luminosity for a neutron star, $\sim 2 \times 10^{38}$ (White, Swank & Holt 1983). For a mass ratio of 0.05 (Rappaport & Joss 1983), this is about 50% greater than the flux required to produce a configuration change provided that the inner Lagrangian point is directly irradiated. Assuming that mass loss occurs through the outer Lagrangian point, we can calculate α from equation (36) to be ~ 460, where x_{L_2} was calculated numerically. Equation (42) then becomes

$$\frac{\dot{P}_{\rm orb}}{P_{\rm orb}} \sim 60\frac{\dot{M}_2}{M_2}. \quad (43)$$

This should be compared to the case where mass transfer is conservative through L_2, where the factor in front of $\dot{M}_2/M_2$ would be ~ 20 instead of 60. Thus, to reproduce the observed rate of orbital decay ($\dot{P}_{\rm orb}/P_{\rm orb} \sim -1.8 \times 10^{-6}$ yr^{-1}), a mass loss rate of around 6.0×10^{-7} M$_\odot$ yr^{-1} through the outer Lagrangian point would be required. This is consistent with the initial rates expected for overflow through the L_1 point in HMXBs during the early phase of mass transfer (e.g. Lamers, van den Heuvel & Petterson 1976). In this case, however, one expects the formation of an *excretion* disc emanating from the L_2 point (see e.g. Shu, Lubow & Anderson 1979), from which emission or absorption lines may be observed depending on the orientation of the observer. Indeed strong evidence for material extending beyond the limiting Roche lobe surface of the secondary has been reported by Mauder (1975) and Clark et al. (1988), although the true origin of this material remains unclear. If indeed the secondary loses mass through the outer Langrangian point, an efficient mechanism would be required to fuel the accretion-powered X-ray source, most likely in the form of a stellar wind, quite likely enhanced by X-ray irradiation (Day & Stevens 1993).

Figure 2 shows approximate equipotential surfaces for Centaurus X-3 for a mass ratio $q = 0.05$. The dotted curve represents the unperturbed Roche lobe, with the compact X-ray source at coordinates (1,0). The dotted inner region represents the deformed secondary when X-ray irradiation (assumed to be Eddington limited) is included, and the L_1 point is shadowed by a thin accretion disc (not shown). The cross-section of the irradiated Roche lobe is significantly reduced by the incident radiation, causing a bottleneck near the L_1 point and strongly reducing the effective cross section for a stream emanating from L_1 (see Lubow & Shu 1975).

If the accretion disc is either tilted or absent, allowing direct irradiation of the L_1 point, the secondary can expand to fill the outer equipotential surface (solid line). Matter will then preferentially escape from the outer Lagrangian point forming an excretion disc (indicated schematically as shaded regions).

If Cen X-3 is losing mass through the outer Lagrangian point, this has several important consequences both for the evolutionary stage of the system and the modelling of the system. Although we use Cen X-3 as an example, the model could apply equally well apply to similar high-luminosity HMXBs, e.g. SMC X-1. We require only that the X-ray flux at the L_1 point is greater than the critical flux; for systems radiating close to the Eddington limit, this will generally be the case.

5.5.1 The lifetime of the X-ray phase

One consequence of mass loss through the outer Lagrangian point is that it may increase the lifetime of the X-ray-active phase of the system. High-luminosity HMXBs are commonly

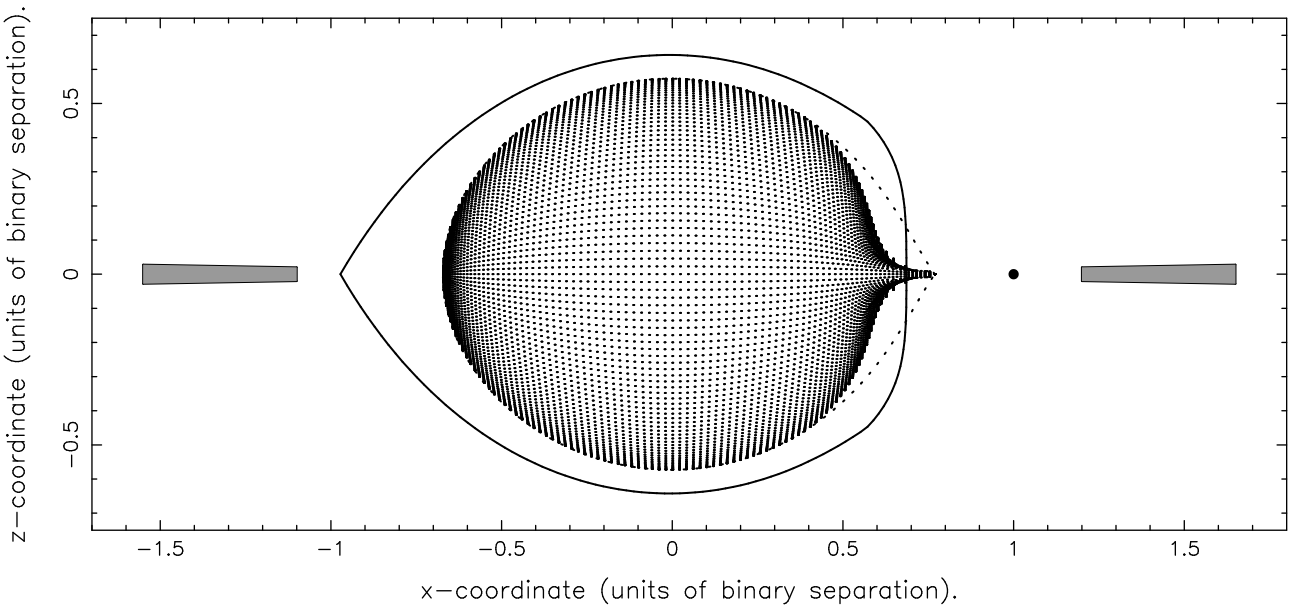

Figure 2. Approximate equipotential surfaces for the high-mass X-ray binary system Centaurus X-3, assuming a mass ratio of 0.05. The dotted curve represents the unperturbed Roche lobe, with the compact X-ray source at coordinates (1,0). The dotted inner region shows the deformed geometry of the critical lobe when the effects of X-ray irradiation are included (for an Eddington-limited X-ray source), but the L_1 point is shadowed by a thin accretion disc (not shown). The thick solid curve shows the critical potential surface when the L_1 is irradiated directly with a luminosity of $2 \times 10^{38}\,\mathrm{erg\,s^{-1}}$. Matter will then preferentially escape from the outer Lagrangian point, forming an *excretion* disc, as indicated schematically by the shaded regions.

assumed to be powered by Roche lobe overflow through the L_1 point (Lamers et al. 1976). However, this will rapidly lead to runaway mass transfer on a thermal time scale, which would result in accretion rates of order 10^{-4} to 10^{-3} $\mathrm{M_\odot yr^{-1}}$ (van den Heuvel & De Loore 1973). Such large rates would quickly and completely extinguish the X-ray source by absorption, suggesting a maximum X-ray lifetime of $\leq 3\times10^3$ yr (Terman, Taam & Savage 1998). In the case of outflow through L_2, all of this mass loss from the secondary will feed a circumbinary disc. The X-ray active lifetime will be determined by the rate at which the wind accretion rate on the neutron star increases. It could be comparable to the lifetime estimated for low-luminosity HMXBs, $\sim 10^4$–10^5 yr, which are thought to be predominantly wind-fed (Meurs & van den Heuvel 1989).

5.5.2 The size of the X-ray eclipse

Cen X-3 is an eclipsing system where the total X-ray eclipse lasts 0.488 d (Schreier et al. 1972), i.e. a fraction of 0.17 of the total period. Defining the eclipse half-angle θ_e as the orbital phase angle at which the occultation of the X-ray source is just complete, the data implies $\theta_\mathrm{e} \approx 42^\circ$. This angle may be directly related to the radius of the secondary R_2 according to

$$\frac{R_2}{a} = (1 - \sin^2 i \cos^2 \theta_\mathrm{e})^{1/2}, \qquad (44)$$

(Rappaport & Joss 1983) where i is the system inclination and a the component separation. If one assumes that the secondary fills its standard Roche lobe, one can then use Eggleton's (1983) expression for the Roche lobe radius to uniquely determine the mass ratio q. Since the mass function is approximately $15\,\mathrm{M_\odot}$ (Schreier et al. 1972), this would yield a mass of the compact object of less than $0.7\,\mathrm{M_\odot}$ (Davidson & Ostriker 1973), which is not consistent with current estimates of ~ 1.4 $\mathrm{M_\odot}$ (e.g. Thorsett et al. 1993) for a typical neutron star. Clark et al. (1988) attempted to fit the Cen X-3 data using a spherically symmetric coronal wind model which took into account the gradual eclipse ingresses and egresses. Their model predicted a more reasonable neutron star mass of 1.23 ± 0.60 $\mathrm{M_\odot}$, but required a much lower (total) eclipse half-angle of 32.9°.

A much simpler solution of this discrepancy is to increase the size of the eclipsing region, as occurs naturally if the secondary is filling it outer critical lobe (see Fig. 2). To demonstrate this, we consider an inclination angle in the probable range 70–80° (Nagase 1989) and assume that neither the star itself nor any material associated with it can exceed the dimensions of the irradiated Roche lobe. Following the analysis of Schreier et al. (1972), we adopt $\theta_\mathrm{e} \approx 45^\circ$ (although Wilson [1972] has suggested values as high as 53°). Equation (44) then implies that the irradiated Roche lobe radius is in the range 0.72–0.75, in units of the orbital separation. Using our model, rather than Eggleton's formula, we relate R_2 to q by calculating the total volume of the irradiated lobe for a given mass ratio and equating this with $\frac{4}{3}\pi R_2^3$. We obtain values for q in the range of 0.101–0.062, which corresponds to a far more plausible range for the neutron star mass of 1.26–1.92 $\mathrm{M_\odot}$. One can expect that a more thorough investigation will yield tighter constraints on the possible masses, the inclination and the eclipse angle.

5.5.3 The optical lightcurve

A second observational problem associated with Cen X-3 is related to the modelling of the optical lightcurve of the sys-

tem (e.g. Mauder 1975; Tjemkes, Zuiderwijk & van Paradijs 1986). Using a standard model for the ellipsoidal variations, Tjemkes et al. (1986) found that the depths of the minima at phases 0.0 and 0.5 were much greater than the typical model parameters predicted. They discounted the possibility of X-ray heating since this would further decrease the depth at phase 0.5. However, Hutchings et al. (1979) presented conflicting evidence. They found the spectral type of the companion star to vary with orbital phase, ranging from O9 near phase 0.0 to O6 near phase 0.5, which strongly suggested appreciable X-ray heating. Our model would appear to broadly reconcile these results if we allow irradiation of the L_1 point, since the initial increase in the companion Roche lobe actually causes an *increase* in this depth due the change in geometry. Clearly, this effect should be included in accurate lightcurve modelling of the system. One should also note that strong irradiation need not necessarily result in a strong 'reflection' effect, since only a fraction of the incident X-ray flux has to be thermalised, while circulation currents will further distribute the heated material around the secondary (Kippenhahn & Thomas 1979; Schandl, Meyer-Hofmeister & Meyer 1997).

5.5.4 Caveats

In our analysis we made two important assumptions: (1) that the secondary is in (almost) synchronous rotation, such that the Roche lobe approximation may be applicable; and (2) that the L_1 point is directly irradiated, with an associated change in the value of the critical potential.

It is generally believed that any initial non-circularity in the binary orbit or frequency difference in the rates of orbital and axial rotation would have been rapidly removed by tides exerted by the compact star on the secondary. The synchronisation timescale in X-ray binaries is generally of the same order of (or shorter than) the circularization time scale (Lecar, Wheeler & McKee 1976; Zahn 1975; Hut 1981). As Fabbiano & Schreier (1977) have shown that the secondary in Cen X-3, also known as Krzeminski's star, is in a highly circular orbit ($e = 0.0008 \pm 0.0001$), it is safe to assume that secondary has synchronized its spin with the orbit.

The second of these caveats is somewhat more problematic. In the simplest model of an X-ray binary, one assumes that matter is accreted onto the compact object through an accretion disc which forms in the orbital plane. The L_1 point is then shadowed from a point-like X-ray source positioned at the compact object. However, there are a several possible alternatives.

First, even if an accretion disc is present, the L_1 point of the secondary may be directly irradiated by X-ray radiation coming from an extended Compton-heated thick accretion disc corona for which evidence has been found in the partial X-ray eclipses of several non-pulsating accretion-powered binary X-ray sources by White & Holt (1982).

Second, the disc plane may be tilted with respect to the binary plane and allow direct irradiation of the secondary (depending on the precession phase). Such tilted discs have variously been proposed to explain precessing discs in systems like Her X-1, LMC X-4 and SS 433 (see e.g. Roberts 1974; Petterson 1977; Priedhorsky & Holt 1987) and even Cen X-3 (Iping & Petterson 1990). As Pringle (1996) has shown, even initially planar discs are unstable to warping due to the external radiation pressure, implying that warping is a generic phenomenon in centrally illuminated accretion discs (also see Maloney & Begelman 1997).

Third, it is by no means clear that an accretion disc forms if mass accretion onto the compact object occurs through a stellar wind, since very little of the orbital angular momentum is actually accreted with the wind material (see e.g. the studies by Ruffert 1994; 1997). No disc is expected to form if the circularization radius, which depends on the specific angular momentum of the accreted material, is less than the Alfvén radius, which defines the radius below which the neutron star's magnetic field will determine the dynamics of the accretion flow.

6 BINARY SYSTEMS CONTAINING AN ACCRETION DISC

In general, LMXBs and some HMXBs contain substantial accretion discs. These shield the inner Lagrangian point from X-ray irradiation, thereby maintaining the relative positions and values of the Lagrangian points. However, radiation pressure may still cause significant deformation of the irradiated stellar surfaces, particularly in systems with high accretion rates. This can change the appearance of the optical lightcurves and radial velocity curves, thereby altering the derived system parameters.

6.1 Observational effects of surface deformations

To illustrate the effects of radiation pressure, we consider a binary system with physical parameters that may be appropriate for the LMXB Scorpius X-1 with an orbital period of 18.9 hr (Kallman, Boroson & Vrtilek 1998), where we take the masses of the neutron star and the secondary to be $1.4\,\mathrm{M}_\odot$ and $1\,\mathrm{M}_\odot$, respectively. The system then has an orbital separation of $4.8\,\mathrm{R}_\odot$. The irradiating X-ray luminosity is assumed to be $2 \times 10^{38}\,\mathrm{erg\,s^{-1}}$, which is approximately the Eddington luminosity of the neutron star. The optical companion in this system is thought to be a Roche-lobe filling star near the end of or just beyond its main-sequence phase (Cowley & Crampton 1975). We take an effective (polar) temperature of 16000K[1], a gravity darkening coefficient of 0.08, and a constant limb-darkening coefficient of 0.35, appropriate to V band observations (see appendix). For the accretion disc, we assume a conservative opening (half) angle of 10° with a fully opaque region of 7°. These parameters imply a mass ratio of $q = 1.4$, and therefore a ratio of radiation to pressure forces $\delta_{\max} = L/qL_{\mathrm{Edd}} \sim 2.5\bar{\kappa}$. Using the approximation described in §4.4, we will assume $\bar{\kappa} = 0.4$, implying $\delta_{\max} = 0.99$. We emphasize that this model should not be considered very realistic, since it makes a number of simplifications, e.g. it assumes constant opacity across the irradiated surface and that all the energy is thermalized below the photosphere of the secondary (i.e. takes a X-ray

[1] This temperature is significantly higher than the effective temperature of a $1\,\mathrm{M}_\odot$ star, but could be appropriate if the secondary were in a similar evolutionary phase as the secondary in Cyg X-2 (Casares, Charles & Kuulkers 1998) or if surface circulation were very efficient in re-distributing the irradiation flux around the secondary

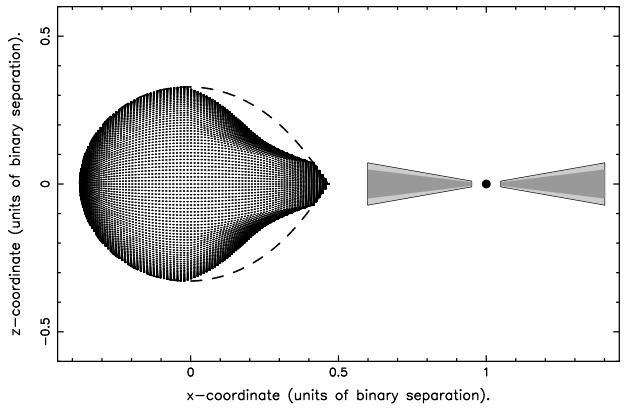

Figure 3. Deformation of the Roche Lobe for $\delta_{\max} = 0.99$, $q = 1.4$. The outline of the standard Roche lobe is shown as a dashed curve, and the X-ray source is represented as a point with coordinates (1,0). The cross-section of the accretion disc is shown containing a heavily shaded opaque region and a more lightly shaded transition region.

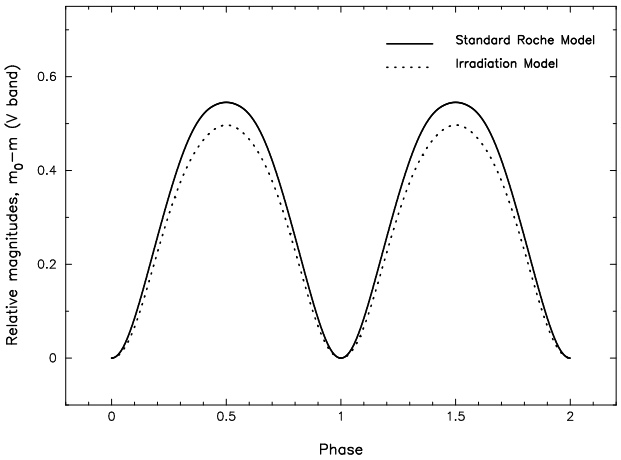

Figure 4. Comparison of V band optical lightcurves due to standard and modified Roche lobes, for the parameters given in the text. Relative magnitudes are calculated by subtracting the theoretical magnitude at each phase, m, from the magnitude at phase 0, m_0.

albedo of 1). The main purpose of the model is to demonstrate the magnitude of the effects of irradiation pressure on the derived system parameters.

The results of the model using these parameters are shown in Figure 3, together with the outline of the Roche lobe due to the standard model. The compact object is again represented as a single point with coordinates (1,0). The cross-section of the accretion disc is shown, containing a heavily shaded opaque region and a more lightly shaded transition region. Its effect as an X-ray shield may be readily inferred from the lack of any distortion around the L_1 point.

The deformation of the Roche surface is very clear. The effect is greatest in the region just beyond the accretion disc shadow, and decreases as the Roche lobe horizon is approached. It should also be noted that the surface equipotentials 'cuts' the interior equipotentials to a depth determined by the extent of the deformation (about 1/5 of the radius for the illustrated case). This may have implications for the circulation of energy along equipotentials.

6.1.1 Effects of radiation pressure on optical lightcurves

To demonstrate the effect of X-ray radiation pressure on optical lightcurves, we have calculated these (using the lightcurve code described in the appendix) for both a standard Roche lobe model and a model with a distorted Roche lobe (Figure 3) for the parameters given above. In order to avoid complications due to eclipses of the secondary or the accretion disc, we chose an inclination of 40°. Figure 4 shows the resulting optical V band lightcurves calculated by summing the flux over the surface of the modified Roche lobe and the standard Roche lobe, respectively. In both cases, the accretion disc is assumed to contribute a fixed amount of flux. For each curve, the relative magnitude is plotted against phase, where the former is calculated by subtracting the theoretical magnitude at each phase, m, from the magnitude at phase 0, m_0. This vertical shift ensures that both curves pass through the origin, thereby highlighting their differences at phase 0.5.

The greatest difference between the two models occurs at phase 0.5, for which the irradiated side of the secondary is most visible and the observed flux is a maximum. The flux due to the pressure-modified lobe is lower, since the distortion results in a decrease in the heated area perpendicular to the line-of-sight. Around phase 0, the curves differ much less, since the backside of the secondary is visible, and its geometry is not affected by radiation pressure.

The amplitude of a lightcurve is defined as the difference in magnitudes between phases 0 and 0.5 and is generally a sensitive function of the inclination of the system. It provides an empirical correlation between the observations and the system parameters (e.g. Bochkarev, Karitskaya & Shakura 1979). If the mass ratio q is known for a system, for example from radial velocity curves determined spectroscopically, it is common to use the lightcurve amplitude to deduce the orbital inclination and with it the component masses, which are proportional to $\sin i$ to the third power. Thus, a fractional error in the value of $\sin i$ propagates to three times this error in the component masses:

$$\frac{\Delta m}{m} \simeq \frac{3\Delta(\sin i)}{\sin i}. \tag{45}$$

The top panel of Figure 5 shows the theoretical amplitudes expected for this system as a function of inclination, calculated for both the standard Roche model and the irradiated model. At an inclination of zero, the observer views the system face-on an no variation in the lightcurve is observed. The amplitude has a maximum at an inclination of 90° when the line-of-sight is parallel to the orbital plane (of course, at large inclination eclipse effects will also strongly affect the lightcurve). As described earlier, the theoretical amplitude is systematically smaller for the irradiated model than in the standard model. Thus, for a given observed amplitude, different models will correspond to different inclinations and hence implied masses (through equ. 45). In the lower panel of Figure 5, we have plotted the quantity $3\Delta \sin i / \sin i$ against inclination, where we assume that the true value of $\sin i$ refers to the irradiation model. This correction is significant (≥ 7 per cent) at all inclinations and rises beyond 30 per cent at the extremes. At an inclination of 40° to the line-of-sight,

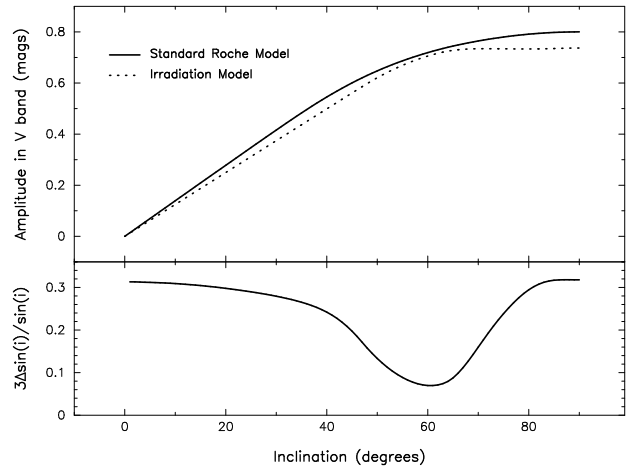

Figure 5. *Top panel*: Theoretical V band amplitudes obtained for the standard Roche model and irradiation model as a function of inclination. *Bottom panel*: The fractional error in $(\sin i)^3$ as a function of inclination. For a given amplitude, the irradiation model is assumed to provide the true inclination.

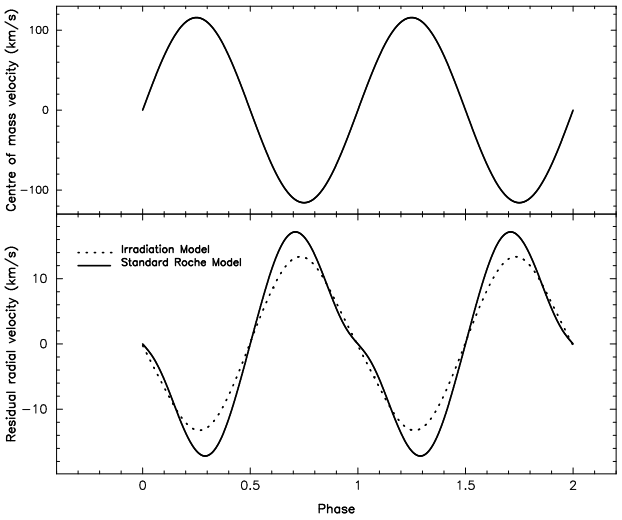

Figure 6. *Top panel:* The radial velocity curve of the centre of mass as a function of phase. *Bottom panel:* The residual radial velocity curves as a function of phase for the standard Roche lobe and radiation pressure model. The relevant parameters are given in the text.

the value of $3\Delta \sin i/\sin i$ is approximately 0.26. implying a $\sim$ 25 per cent error in the component masses. At lower inclinations, the error is greater still.

Systems where external radiation pressure can be expected to be important are systems such as Scorpius X-1, Cygnus X-2 or the black hole candidate GRO J1655-40, in which the secondary is sufficiently evolved so as to allow optical observations during outburst (Orosz & Bailyn 1997). The effect will also be of importance in HMXBs, whose optical output is dominated by the high-mass secondary star (for example, the super-Eddington X-ray binary, LMC X-4; see Heemskerk & van Paradijs 1989).

6.1.2 Effects of radiation pressure on radial velocity curves

The distortion of the secondary also affects the interpretation of radial velocity curves obtained from the phase-dependent Doppler shifts of spectral lines. In the presence of irradiation, the temperature of the heated side of the secondary may be increased by a factor of 2 or more, depending on the type of system and X-ray luminosity. This causes phase-dependent asymmetries in the shapes of individual spectral lines and shifts the effective velocity centre of the lines. If these effects are not properly taken into account, this leads to incorrect determinations of the radial velocity amplitude (see Wade & Horne 1988; Shahbaz & Wood; Phillips, Shahbaz & Podsiadlowski 1999). The deformation of the Roche lobe introduces a further higher-order error. In order to illustrate the magnitude of these effects, we consider flux-weighted *residual* radial velocity curves calculated using the same system parameters as above (with $M_1 = 1.4\,\mathrm{M}_\odot$, $M_2 = 1\,\mathrm{M}_\odot$, $P_{\rm orb} = 18.9\,\mathrm{hr}$, $L_x = 2 \times 10^{38}\,\mathrm{erg\,s^{-1}}$).

The lower panel of Figure 6 shows the residual radial velocity curves calculated with these parameters and an inclination of 40° for a model that includes only the variation of the surface temperature (including irradiation) and a model that includes the effects due to the temperature variation and the surface distortion. Here, the residual velocity was calculated according to

$$V_{\rm resid}(\Phi, i) = \frac{\sum_{r,\theta,\phi} V_{\rm rad}(r,\theta,\phi,\Phi,i)\Delta F(r,\theta,\phi,\Phi,i)}{\sum_{r,\theta,\phi} \Delta F(r,\theta,\phi,\Phi,i)} - V_{\rm rad}^{\rm CM}(\Phi,i), \quad (46)$$

where $V_{\rm rad}(r,\theta,\phi,\Phi,i)$ is the radial velocity for a given orbital phase angle Φ and inclination i at a grid point (r,θ,ϕ), $\Delta f(r,\theta,\phi,\Phi,i)$ is the observed flux for a given surface element, and $V_{\rm rad}^{\rm CM}(\Phi,i)$ is the centre-of-mass radial velocity of the secondary. (The summation is only performed over the visible area of the star.)

At phase 0, the observer sees the backside of the secondary, and the radial velocity (and residual radial velocity) is zero. The radial velocity increases and becomes positive as the secondary moves away from the observer. However, the heated face of the secondary is now visible, and this shifts the 'effective centre' of the velocity towards the centre of mass of the binary orbit. Hence the radial velocity is reduced and the residual radial velocity is negative. It falls to zero once more at phase 0.5, when the heated face of the secondary is directly in the observer's line-of-sight. After phase 0.5, the secondary moves back towards the observer and so the reverse effect is seen. The amplitude of these effects is substantially smaller (by about 30% or ~ 4 km s^{-1}) for the pressure modified surface compared with the standard Roche lobe. Again, this is a consequence of the decrease in the projected heated area perpendicular to the observer's line of sight, due to the deformation of the surface. This demonstrates that the distortion of the surface reduces the K correction that needs to be applied to obtain the true underlying radial velocity curve. This will be particularly important for systems like Sco X-1, where the measured X-ray luminosity ($\sim 1.8 \times 10^{38}$ erg s^{-1}; Kallman et al. 1998) indicates strong heating at phase 0.5.

7 CONCLUSIONS

We have shown that irradiation of the secondary in a close binary can have a significant influence on the shape of irradiated stellar surfaces and on system configurations. We have constructed approximate numerical solutions of the equipotential surfaces of secondaries where external irradiation effects are important to demonstrate the main physical effects. These generally scale with the luminosity of the radiation source and become dramatic whenever the ratio of radiation to gravitational forces approaches the critical value. The inclusion of the radiation pressure term in the total effective potential leads to considerable deviations from the standard Roche geometry. Depending on the luminosity of the radiation source and the relative efficiency of absorption in the irradiated photosphere, the most important effects are:

(1) The geometry of the equipotential surface in the vicinity of the irradiated region is altered, in particular for high X-ray luminosities.

(2) For systems without accretion discs, the position of the irradiated inner Lagrangian (L_1) point is shifted. This leads to an increase in the size of the critical Roche lobe.

(3) When the irradiating luminosity increases above a critical value, the (irradiated) inner Lagrangian point ceases to be the Lagrangian point with the lowest potential. Then the critical potential will be set by the L_2 point (or the L_3 point in HMXB's) and an outer critical configuration will be obtained.

(4) In such outer critical configurations, mass loss occurs through the outer Lagrangian point. This may influence the evolutionary processes of systems such as binary pulsars or stars orbiting supermassive black holes in AGN.

(5) In the case of mass loss purely from the L_2 point, the associated change in angular momentum can lead to self-sustaining mass loss. This may be relevant for binary systems which show a steady decay in orbital period, and may lengthen the stable lifetimes of some HMXBs. Centaurus X-3 would appear to be a possible candidate.

(6) Due to the deformation of the stellar surface, lightcurves and radial velocity curves in LMXBs and HMXBs are modified. These effects need to be included for a reliable determination of system parameters.

Finally, we note that while it has yet to be demonstrated conclusively that radiation pressure can effect the global structure of a star to the extent proposed in this paper, it is clear that the pressure force due to external irradiation can be of a considerable magnitude. No analysis of high-luminosity X-ray binary systems can be complete without an adequate treatment of these effects.

APPENDIX : THE OPTICAL LIGHTCURVE CODE

Surface Geometry:

The secondary is modelled using a surface modified by irradiation pressure with the assumptions of synchronous rotation and a circular orbit. The surface is then divided into grid points spaced equally in $\cos\theta$ and ϕ. The accretion disc is modelled as described in §4.2.2.

Gravity-Darkening:

Von Zeipel's (1924b) theorem provides a relationship between the local potential gradient and the local emergent flux f in a tidally or rotationally distorted star in radiative equilibrium, $f_{\rm rad} = \sigma T^4 \propto |\boldsymbol{\nabla}\Omega|$. Consequently, the temperature at any point on the star is given by

$$\frac{T(x,y,z)}{T_{\rm pole}} = \left[\frac{|\boldsymbol{\nabla}\Omega|(x,y,z)}{|\boldsymbol{\nabla}\Omega|_{\rm pole}}\right]^{\beta}, \qquad (1)$$

where $T_{\rm pole}$ and $|\boldsymbol{\nabla}\Omega|_{\rm pole}$ are the temperature and potential gradient at the pole of the star. The gravity darkening exponent β has two values: 0.25 for stars with radiative atmospheres (von Zeipel 1924b), and 0.08 for stars with fully convective envelopes (Lucy 1967).

Limb-Darkening:

For each grid point on the secondary surface, the temperature obtained from gravitational darkening is used to compute the monochromatic intensity according to Planck's relation:

$$I(\lambda,T) \propto \left[\exp\left(hc/k\lambda T\right) - 1\right]^{-1}. \qquad (2)$$

This intensity is modified using a standard linear limb-darkening law,

$$I(\mu) = I(1)\{1 - u + u\cos\gamma\}, \qquad (3)$$

where γ is the angle of foreshortening, and $\mu = \cos\gamma$. $I(\mu)$ represents the distribution of the emergent intensity which varies with the angle of foreshortening. The limb-darkening coefficients u are taken from standard tables computed from model atmospheres (e.g. Al Naimiy 1978). See Kopal & Kitamura (1968) and Avni (1978) for more discussions on these approximations.

X-ray Heating:

The X-ray flux that each surface element intercepts is given by

$$f_{\rm X-ray}(x,y,z) = \frac{L_{\rm x}}{4\pi d^2(x,y,z)}\cos\epsilon(x,y,z), \qquad (4)$$

where $L_{\rm x}$ is the luminosity of the source, d the distance from the element to the source, and ϵ the angle of foreshortening. Assuming total thermalisation of the incident radiation, we can determine the modified temperature of each surface element visible from the source (i.e. for which $\cos\epsilon > 0$) from

$$T^4_{\rm X-ray}(x,y,z) = T^4_{\rm pole}\left(\frac{|\boldsymbol{\nabla}\Omega|(x,y,z)}{|\boldsymbol{\nabla}\Omega|_{\rm pole}}\right)^{4\beta} + \frac{(1-W)f_{\rm X-ray}(x,y,z)}{\sigma}, \qquad (5)$$

where W is the albedo, and σ the Stefan constant.

We now have a grid of temperature values over the secondary surface from which we can calculate the total luminosity and flux. This calculation is repeated in steps of the phase angle. Optical lightcurves and flux-weighted radial velocity curves may then be calculated.

REFERENCES

Al Naimiy H.M., 1978, Ap&SS, 53, 181
Artymowicz P., Clarke C.J., Lubow S.H., Pringle J.E., 1991, ApJ, 370, L35
Avni Y., 1978, in Giacconi R., Ruffini R., eds, Physics and Astrophysics of Neutron Stars and Black Holes, North-Holland, Amsterdam, p. 42
Bochkarev N.G., Karitskaya E.A., Shakura N.I., 1979, Astron. Zh., 56, 16
Casares J., Charles P., Kuulkers E., 1998, ApJL, 493, L39
Charbonneau P., 1992, A&A, 259, 134
Clark G.W., Minato J.R., Guozhu, M., 1988, ApJ, 324, 974
Cowley A.P., Crampton, D., 1975, ApJ, 201, L65
Darwin G.H., 1879, Proc. R. Soc. Lond., 29, 168
Davidson K., Ostriker J.P., 1973, ApJ, 179, 585
Davey S., Smith R.C., 1992, MNRAS, 257, 476
Day C.S.R., Stevens I.R., 1993, ApJ, 403, 322
Drechsel H., Haas S., Lorenz R., Gayler S., 1995, A&A, 294, 723
Eggleton P.P., 1983, ApJ, 268, 368
Fabbiano G., Schreier E.J., 1977, ApJ, 214, 235
Fabian A.C., 1992, in Frontiers of Astrophysics, University Academy Press, Tokyo, p. 603
Frank J., King A.R., Raine, D.J., 1992, in Accretion Power in Astrophysics, 2nd edn., CUP, Cambridge
Fruchter A.S., Stinebring D.R., Taylor, J.H., 1988, Nat, 333, 237
Fruchter A.S., et al., 1990, ApJ, 351, 642
Heemskerk M.H.M., van Paradijs J., 1989, A&A, 223, 154
Hut P., 1981, A&A, 99, 126
Hutchings J.B., Cowley A.P., Crampton D., van Paradijs J., White N.E., 1979, ApJ, 229, 1079
Iping R.C., Petterson J.A., 1990, A&A, 239, 221
Kallman T., Boroson B., Vrtilek S.D., 1998, ApJ, 502, 441
Kelley R.L., Rappaport,S., Clark G.W., Petro L.D., 1983, ApJ, 268, 790
Kippenhahn R., Thomas H.C., 1979, A&A, 75, 281
Kondo Y., McCluskey G.E., 1976, in Eggleton P.P. et al., eds, IAU Symp. 73, Structure and Evolution of Close Binary Systems, Reidel, Dordrecht, p. 277
Kopal Z., 1959, Close Binary Systems, Wiley
Kopal Z., 1988, Ap&SS, 144, 557
Kopal Z., Kitamura K., 1968, Adv. Astron. Astrophys., 6, 125
Kruszewski A., 1966, Adv. Astron. Astrophys., 4, 233
Lamers H.J.G.L.M., van den Heuvel E.P.J., Petterson J.A., 1976, A&A, 49, 327
Lecar M., Wheeler J.C., McKee C.F., 1976, ApJ, 205, 556
Levine A., Rappaport S., Deeter J.E., Boynton P.E., Nagase F. 1993, ApJ, 410, 328
Lubow S.H., Shu F.H., 1975, ApJ, 198, 383
Lucy L.B., 1967, Z.Ap., 65, 89
Lyne A.G., Johnston S., Manchester R.N., Staveley-Smith L, D'Amico N., 1990, Nat, 347, 650
Nagase F., 1989, PASJ, 41, 1
Maloney P.R., Begelman M.C., 1997, ApJL, 491, L43
Martin T.J., Davey S.C., 1995, MNRAS, 275, 31
Maeder A., Zahn J.P., 1998, A&A, 334, 1000
Mauder H., 1975, ApJ, 195, L27
McCormick P., Frank J., 1993, BAAS, 182, 6409
Meurs E.J., van den Heuvel E.P.J., 1989, A&A, 226, 88
Orosz J.A., Bailyn C.D., 1997, ApJ, 477, 876
Osaki Y., 1982, PASJ, 34, 257
Peraiah A., 1982, JApA, 3, 485
Petterson J.A., 1977, ApJ, 216, 827
Phillips S.N., Shahbaz T., Podsiadlowski Ph., 1999, MNRAS, 304, 839
Plavec M.J., 1958, Mem. Soc. R. Sci. Liège, 20, 411
Podsiadlowski Ph., 1991. Nature, 350, 136
Podsiadlowski Ph. 1992, in Kondo, Y., Sisteró, R. F., & Polidan, R. S., eds, IAU Symp. No. 151, Evolutionary Processes in Interacting Binaries, Kluwer, Dordrecht, p. 457
Podsiadlowski Ph., Rees M.J., 1994, in Holt S.S., Day, C.S., eds, AIP Conference: Evolution of X-Ray Binaries, AIP, New York, p. 71
Press, W. H., Teukolsky, S. A., Vetterling, W. T., Flannery, B. P. 1992, Numerical Recipes in Fortran: the Art of Scientific Computing (Cambridge: Cambridge University Press), Chapter 9.4
Priedhorsky W.C., Holt S.S., 1987, Space Sci. Rev., 45, 291
Pringle J.E., 1974, MNRAS, 168, 13p
Pringle J.E., 1996, MNRAS, 281, 357
Rappaport S., Joss, P.C., 1983, in Lewin W.H.G., van den Heuvel E.P.J., eds, Accretion-driven Stellar X-Ray Sources, CUP, Cambridge, p. 1
Rappaport S., Verbunt F., Joss P.C., 1983, ApJ, 275, 713
Rees M.J., 1984, ARA&A, 22, 471
Ritter H., 1996, in Wijers, M.J., Davies, M.B., & Tout, C.A., eds, Evolutionary Processes in Binary Stars, Kluwer, Dordrecht, p. 223
Roberts W.J., 1974, ApJ, 187, 575
Ruderman M., Shaham J., Tavani M., 1989, ApJ, 336, 507
Ruffert M., 1994, A&AS, 106, 505
Ruffert M., 1997, A&A, 317, 793
Schandl S., Meyer-Hofmeister E., Meyer F., 1997, A&A, 318, 73
Schreier E., Levinson R., Gursky H., Kellogg E., Tananbaum H., Giacconi R., 1972, ApJ, 172, L79
Schuerman D.W., 1972, Ap&SS, 19, 351
Shahbaz T., Wood J.H., 1996, MNRAS, 282, 362
Shu F.H., Lubow S.H., Anderson L., 1979, ApJ, 229, 223
Terman J.L., Taam R.E., Savage C.O., 1998, MNRAS, 293, 113
Thorsett S.E., Arzoumanian Z., McKinnon M.M., Taylor J.H., 1993 ApJ, 405, L29
Tjemkes S.A., Zuiderwijk E.J., van Paradijs, J., 1986, A&A, 154, 77
van den Heuvel, E.P.J., De Loore, C., 1973, A&A, 25, 387
van Paradijs J., 1998, in Buccheri R., van Paradijs J., Alpar M.A., eds, The Many Faces of Neutron Stars, Kluwer, Dordrecht, p. 279
Vanbeveren D., 1977, A&A, 54, 877
Von Zeipel H., 1924a. in Kienle H., ed., Probleme der Astronomie, Festschrift für H. v. Seeliger, Springer, Berlin, p. 144
Von Zeipel H., 1924b, MNRAS, 84, 665
Wade R.A., Horne K., 1998, ApJ, 324, 411
Wilson R.E., 1972, ApJ, 174, L27
White N.E., Holt S.S., 1982, ApJ, 257, 318
White N.E., Swank J.H., Holt, S.S., 1983, ApJ, 270, 711
Zahn J.P., 1975. A&A, 41, 329
Zhou H.N., Leung K.C., 1988, Ap&SS, 141, 257